Open channel noise

VI. Analysis of amplitude histograms to determine rapid kinetic parameters

Stefan H. Heinemann* and Frederick J. Sigworth‡

*Max-Planck-Institut für biophysikalische Chemie, Abteilung Membranbiophysik, D-3400 Göttingen, Germany; and ‡Department of Cellular and Molecular Physiology, Yale University School of Medicine, New Haven, Connecticut 06510 USA

ABSTRACT Recently we reported that rapid fluctuations of ion currents flowing through open gramicidin A channels exceed the expected level of pure transport noise at low ion concentrations (Heinemann, S. H. and F. J. Sigworth. 1990. *Biophys. J.* 57:499–514). Based on comparisons with kinetic ion transport models we concluded that this excess noise is likely caused by current interruptions lasting ~1 μs. Here we introduce a method using the higher-order cumulants of the amplitude distribution to estimate the kinetics of channel closing events far below the actual time resolution of the recording system. Using this method on data recorded with 10 kHz bandwidth, estimates for gap time constants on the order of 1 μs were obtained, similar to the earlier predictions.

INTRODUCTION

The investigation of fast kinetic processes in ion channels, such as structural fluctuations that modulate the ion current, is subject to the limited time resolution of the recording system. Several strategies have been used to analyze brief closing events that are beyond the actual time resolution. One approach is to fit reconstructed, theoretical closing events to the measured, not fully resolved signals (Colquhoun and Sigworth, 1983). Another is to compute the power spectrum of the channel recording (Colquhoun and Ogden, 1988; Sine et al., 1990); in cases where the necessary recording bandwidth can be obtained, fits to Lorentzian components in the spectrum can yield estimates of time constants even when the background noise obscures individual open-closed transitions. A third strategy makes use of the amplitude distributions of the recorded current. FitzHugh (1983) has shown that the amplitude distribution of a recording from a two-state channel, filtered with a simple first-order filter, is a beta function. Yellen (1984) subsequently found that the beta function also describes well the distributions obtained from recordings with higher-order filters, and he and others (e.g., Pietrobon et al., 1989) have thus been able to determine dwell times that are shorter than the risetime of the recording system by fitting the experimental amplitude distributions.

We have used a variant of the power-spectrum approach in three studies of open-channel noise in gramicidin A (GA) channels (Heinemann and Sigworth, 1988, 1989, 1990). In these studies only the low-frequency asymptote of the power spectrum was measurable, so that direct estimates of time constants from corner frequencies could not be made. Instead we used the ionic concentration dependence of the spectral density and the mean channel current to determine kinetic parameters in specific models for ion permeation. Basically the idea was that by varying ion concentrations we could vary specific rates in the process of ion permeation; the effect of these rates on the fluctuations would depend on the mechanism and time scale of the fluctuations. In the first two of these studies we used this approach to estimate the residence times for formamide and Na^+ in the GA channel, obtaining values of ~100 and ~10 ns, respectively. Relatively noisy currents through GA channels are seen in the absence of blocking ions when K^+ and Cs^+ are the charge carriers. In the third study we found that the concentration dependence of the spectral density could best be explained by fluctuations in the entry rate of ions into the empty channel, occurring on a time scale of roughly 1 μs.

The goal of the work described here is to provide independent estimates for the duration and rates of the brief interruptions in Cs^+ current predicted by the model of open-channel noise in this last study (Heinemann and Sigworth, 1990). For this we analyze the amplitude distribution of the recorded current while a gramicidin channel is conducting. The theory we present here is based on a limiting case in which the brief current interruptions (gaps) under study occur rarely and are very much shorter than the response time of the recording system. These assumptions allow us to treat the amplitude distribution of the recorded signal as a Gaussian function with a small, skewed contribution due to the gaps. This contribution can be characterized by

0006-3495/91/09/577/11 $2.00

the cumulants (linear combinations of moments of the distribution), whose values are predicted from the impulse response of the recording system and the distribution of durations of the gaps. With the theory presented here and given the cumulants of an experimental amplitude distribution, one can obtain estimates for the rate and duration of brief closures. Our analysis of the cumulants of "shot" events arising from brief closures parallels the analysis by Fesce et al. (1986) of the higher moments of endplate currents in studying quantal events.

THEORY

Review of moments and cumulants

The nth moment of a distribution $f(x)$ about zero is defined as:

$$\mu'_n = \int_{-\infty}^{\infty} f(x)^n \, dx. \quad (1)$$

From the μ'_n the nth moment μ_n about the mean of the distribution can be obtained as

$$\mu_n = \sum_{j=0}^{n} \binom{n}{j} \mu'_{n-j} (-\mu'_1)^j. \quad (2)$$

The cumulants κ_n are linear combinations of the moments. They are also called "semi-invariants" in the literature. They have the important property that if x and y are independent random variables, the n^{th} cumulant of the distribution of $x + y$ will be equal to the sum of the n^{th} cumulants of x and y alone. It is well known that the mean and variance satisfy this property, and in fact these are equal to κ_1 and κ_2, respectively. In general the κ_n are given by the coefficients of an expansion of the distributions's characteristic function $\phi(t)$, as are the μ_n, so their relationship can be expressed by the identity (Kendall, 1947)

$$\phi(t) = \sum_{j=0}^{\infty} \frac{\mu_j (it)^n}{n!} = \exp\left\{\sum_{j=1}^{\infty} \frac{\kappa_j (it)^n}{n!}\right\} \quad (3)$$

with $i = \sqrt{-1}$. The first cumulants are

$$\begin{aligned} \kappa_2 &= \mu_2 \\ \kappa_3 &= \mu_3 \\ \kappa_4 &= \mu_4 - 3\mu_2^2 \\ \kappa_5 &= \mu_5 - 10\mu_3\mu_2 \\ \kappa_6 &= \mu_6 - 15\mu_4\mu_2 - 10\mu_3^2 + 30\mu_2^3 \\ \kappa_7 &= \mu_7 - 21\mu_5\mu_2 - 35\mu_4\mu_3 + 210\mu_3\mu_2^2. \end{aligned} \quad (4)$$

Cumulants of shot events

If we assume for now that the open-channel current is noiseless we can picture brief closings of the open channel as events creating a shot noise. Let the deviation from the steady open-channel current level be composed of individual current pulses with the normalized time course $\zeta(t)$ and amplitude y. The pulses are assumed to arise from a Poisson process, which means that the occurrence of each pulse is independent of the others; let the mean frequency of occurrence be λ. In this case the cumulants of the distribution generated by this shot process are proportional to λ and can be calculated according to the general Campbell theorem (Campbell, 1909),

$$\kappa_n = \lambda y^n I_n, \quad (5)$$

where

$$I_n = \int_{-\infty}^{\infty} \zeta(t)^n \, dt. \quad (6)$$

Thus, given a known time course of the individual events, their frequency and amplitude can be determined from the ratios of successive cumulants:

$$y = \frac{\kappa_n}{\kappa_{n-1}} \frac{I_{n-1}}{I_n} \quad (7)$$

and

$$\lambda = \frac{\kappa_{i-1}^{i} I_n^{n-1}}{\kappa_i^{i-1} I_{n-1}^{n}}. \quad (8)$$

It should be noted that brief gaps in channel currents do not occur as a Poisson process, even when they arise from simple two-state kinetics. This is because the gaps have finite duration and the renewal time is the sum of that duration and the time between gaps. We assume here that the gap duration is very small compared with the inter-gap time. This is equivalent to picturing the gaps as being independent current pulses that are so brief that, when they are superposed, the probability of overlap is negligible. With the further assumption that the inter-gap times are exponentially distributed, the gap process approaches Poisson behavior.

Campbell's theorem can be extended if the amplitudes y of the events are variable (Rice, 1954):

$$\kappa_n = \lambda \langle y^n \rangle I_n, \quad (9)$$

where $\langle y^n \rangle$ is the ensemble average of the nth power of the distribution of y, which is *de facto* the nth moment about zero of that distribution:

$$\langle y^n \rangle = \int_{-\infty}^{\infty} y^n f_y(y) \, dy. \quad (10)$$

Cumulants of events having exponentially distributed durations

Let the unitary events be square pulses with a constant amplitude y_0 and exponentially distributed duration with mean τ. When these events are filtered by the limited resolution of the recording system, they result in small inflections in the recorded signal, and a small, skewed component near y_0 in the amplitude distribution (Fig. 1). To compute the cumulants of this component we first consider the effect of filtering on the signal. The measured signal due to a rectangular pulse of duration w may be formally described by

$$y(t, w) = y_0[H(t) - H(t - w)], \tag{11}$$

where $H(t)$ is the step response function of the system and y_0 the amplitude of the event. Since we consider pulses of short duration only, (Eq. 11) can be expanded into a Taylor series:

$$y(t, w) = y_0[w(H'(t) - w^2H''(t) + \cdots], \tag{12}$$

where the primes denote time derivatives. Taking only the term that is linear in w we have

$$y(t, w) \approx y_0wh(t), \tag{13}$$

where $h(t) = H'(t)$ is the impulse response of the recording system.

Thus in the limit of small durations w the response to a rectangular pulse always has the time course $h(t)$ but with an amplitude that is proportional to w. Let w be exponentially distributed, i.e., have the probability density

$$f_w(w) = \frac{1}{\tau}e^{-w/\tau} \tag{14}$$

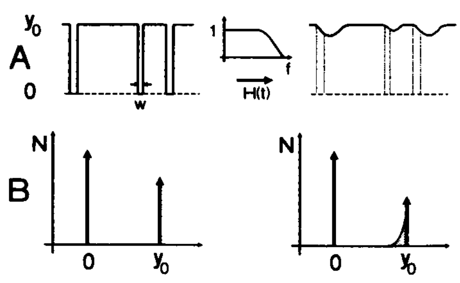

FIGURE 1 (*A*) Brief channel closing events are observed as weak inflections of the open-channel current after filtering (*right side of the figure*). (*B*) The histogram of current amplitudes near the open-channel current y_0 becomes skewed (*shaded region*) if the brief channel closings are not fully resolved. The skew of the histogram and the higher moments provide information about the underlying kinetic process.

then the probability density function of amplitudes y of the filtered signal is

$$f_y(y) = \alpha e^{-\alpha y}, \tag{15}$$

where $\alpha = 1/(y_0\tau)$. Using Eqs. 9 and 10 we then obtain for the cumulants of the amplitude distribution of the filtered signal

$$\kappa_n = \lambda \int_0^\infty y^n \alpha e^{-\alpha y}\, dy \int_{-\infty}^\infty h^n(t)\, dt. \tag{16}$$

This equation gives, then, the cumulants arising from events operated on by a filter with any impulse response $h(t)$. For application to our data we assume a Gaussian filter characteristic with cutoff frequency f_c. This is the form of digital filter we use for our data, and is a good approximation to the response of a high-order Bessel filter. The impulse response of a Gaussian filter is (Colquhoun and Sigworth, 1983):

$$h(t) = \frac{1}{\sqrt{2\pi}\sigma} e^{-t^2/2\sigma^2}, \tag{17}$$

with

$$\sigma = \frac{\sqrt{\ln 2}}{2\pi f_c}. \tag{18}$$

Incorporating this into Eq. 16 yields the expression for the cumulants

$$\kappa_n = \lambda \int_0^\infty y^n \alpha e^{-\alpha y}\, dy \int_{-\infty}^\infty \left[\frac{1}{\sqrt{2\pi}\sigma} e^{-t^2/2\sigma^2}\right]^n dt. \tag{19}$$

The integrals have simple solutions

$$\kappa_n = \lambda \frac{n!}{\sqrt{n}} \frac{(\sqrt{2\pi}\sigma)^{1-n}}{\alpha^n} \tag{20}$$

which, after substituting for α and σ, yield

$$\kappa_n = \lambda \frac{n!}{\sqrt{n}} y_0^n \tau^n \left(\frac{\sqrt{\ln 2}}{\sqrt{2\pi} f_c}\right)^{1-n} \tag{21}$$

From these expressions τ and λ can be derived, by analogy to Eqs. 7 and 8,

$$\tau = \frac{\kappa_n}{\kappa_{n-1}} \frac{1}{\sqrt{n(n-1)}} \frac{1}{y_0} \frac{\sqrt{\ln 2}}{\sqrt{2\pi} f_c} \tag{22}$$

$$\lambda = \frac{\kappa_{n-1}^n}{\kappa_n^{n-1}} \frac{(n-1)^{n/2} n^{(n+1)/2}}{n!} \frac{\sqrt{2\pi} f_c}{\sqrt{\ln 2}}. \tag{23}$$

Thus we see that values of τ and λ can be obtained by taking the ratios of successive cumulants.

Cumulants from open-channel noise

In the analysis of open-channel noise in GA channels the unitary events that we consider are brief gaps in the channel current. In addition to these fluctuations there is noise from more rapid steps in the ion-permeation process and there is background noise from the recording amplifier, thermal noise in the pipette, etc. The background noise makes the largest contribution, but it is readily measured during the periods when no channels are open and is seen experimentally to be Gaussian distributed. We expect it to be uncorrelated with the open-channel noise, and experimental tests are consistent with this (Sigworth et al., 1987), so that we can simply subtract the cumulants of the background noise alone from the cumulants of the open-channel amplitude distribution.

The noise from rapid ion-transport steps is a more difficult problem. In the previous papers of this series we have modeled the ion-permeation process as a Markov process in which transitions among states result in delta functions of current as ions move among sites in the channel. The specific scheme used here and in the previous paper (Heinemann and Sigworth, 1990) is based on the two-site, three barrier model of Urban et al. (1980). That model has been quite successful in explaining conductance-activity relations, flux ratio measurements, and mole-fraction effects that have been observed in gramicidin A channels (see Andersen, 1984, for a review). (More elaborate schemes that also allow double occupancy of the channel [e.g., Sandblom et al., 1983] have been shown to be superior in some respects, but we did not consider these because of the computational complexity.) We extended the two-site, three-barrier model to include an extra "blocked" state of the unoccupied channel (Fig. 2 *A*). This allowed it to explain the relatively large open-channel noise observed at low concentrations of some permeant ions, particularly Cs^+ (Heinemann and Sigworth, 1990). Other schemes, such as the "gating" model in Fig. 2 *B*, predict very different concentration dependences of the spectral density which were not consistent with our experimental results.

In our previous paper we computed the spectral density of open-channel noise by applying the theory of Frehland (1978, 1982) to the entire kinetic scheme in Fig. 2 *A*. In the present study we make an approximation, taking advantage of the fact that the blocked state [00]* appears to have a lifetime on the order of 1 μs, an order of magnitude longer than any other state in the scheme. The current through the channel can be pictured as delta functions of current (mainly due to the ion translocation transitions between the states [IO] and [OI]) occurring about every 30 ns at 500 mM Cs^+. There is considerable noise from these transport events, but

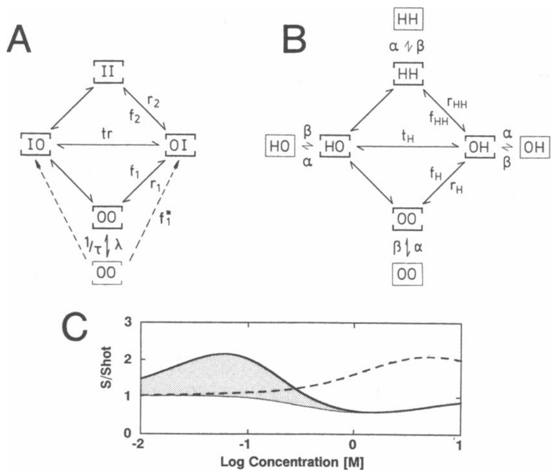

FIGURE 2 State diagrams and spectral density of the open-channel noise. The state diagrams are based on the two-site, three-barrier model (see Finkelstein and Andersen, 1981) which is shown highlighted here. (*A*) The state diagram is extended by an extra channel-empty state [00]* to model fluctuating entry barriers. (*B*) An example of an alternative model, one considered by Frehland (1982), in which channel "gating" can occur in any state of ion occupancy, but in which ion motions are frozen while the channel is "closed." (*C*) Predictions of the spectral density normalized to the classical shot noise $S_{shot} = 2iq$ as a function of ion concentration. The thin line is ion-transport noise in the basic four-state transport model; the heavy line is the fluctuating barrier model (as in part *A*); and the dashed line is simple gating (as in part *B*). In our previous paper we found that the concentration dependence of the spectral density is well described by the scheme in *A*.

because they occur so rapidly the current pulses will be filtered enough to result in an essentially Gaussian-distributed noise. During the gaps, which represent dwells in the blocked state, this noise is transiently stopped; however, since even the gap times are short compared with the response time of the recording system, the absence of the noise during the gaps is a higher-order effect that we expect to be small and will ignore. Thus we model the fluctuations from the rapid transport events as simply an independent, Gaussian-distributed noise component that is added to the fluctuations due to the gaps. This model greatly simplifies the analysis. For a Gaussian distribution the cumulants of order 3 or higher are zero; thus only the fluctuations from brief gaps should contribute to κ_3 and the higher cumulants.

Statistical error in moments and cumulants

The contribution to the moments (at least to the even moments) of the brief gaps is expected to be very small compared with the contribution from the background noise. The statistical errors in the cumulants will therefore depend strongly on the amount of background noise. We calculate here the variance of estimates of the moments and cumulants due to Gaussian background noise. The estimates can then be used to gauge the reliability of the values of the cumulants obtained from the experimental data.

Consider an amplitude histogram obtained from a large number of independent samples, having n_j events in the jth bin. Let the mean of the distribution be zero. The total number of events is

$$N = \sum_{j=1}^{n_b} n_j \tag{24}$$

with the number of bins being n_b. The moments are calculated as:

$$\mu_i = \frac{1}{N} \sum_{j=1}^{n_b} j^i n_j. \tag{25}$$

Independent samples implies that the n_j are Poisson-distributed, so that their variance is:

$$\mathrm{var}(n_j) = n_j. \tag{26}$$

The variance of the moments of index i is then given by

$$\begin{aligned} \mathrm{var}(\mu_i) &= \frac{1}{N^2} \sum_j j^{2i} \mathrm{var}(n_j) \\ &= \frac{1}{N^2} \sum_j j^{2i} n_j \\ &= \frac{1}{N} \mu_{2i}. \end{aligned} \tag{27}$$

Because Gaussian background noise dominates our experimental distributions, we will compute the variance assuming a Gaussian distribution. The first moments about the mean of a Gaussian distribution are

$$\mu_1 = \mu_3 = \mu_5 = \cdots = 0 \tag{28}$$

and

$$\mu_{2k} = \sigma^{2k} \prod_{j=1}^{k} (2j - 1), \quad k = 1, 2, 3, \ldots \tag{29}$$

The variances for the moments of a Gaussian distribution are therefore

$$\begin{aligned} \mathrm{var}(\mu_k) &= \frac{1}{N} \mu_{2k} \\ &= \frac{1}{N} \sigma^{2k} \prod_{j=1}^{k} (2j - 1). \end{aligned} \tag{30}$$

The variances of the cumulants can be evaluated in a similar fashion from the general expression

$$\mathrm{var}(\kappa_i) = \sum_j \left(\frac{\partial \kappa_i}{\partial n_j}\right)^2 n_j, \tag{31}$$

where again we have made use of the fact that $\mathrm{var}(n_j) = n_j$ for Poisson-distributed n_j. For a distribution of N Gaussian-distributed samples with variance σ^2 the variances of the cumulants so obtained are:

$$\begin{aligned} \mathrm{var}(\kappa_2) &= \frac{3}{N} \sigma^4 \\ \mathrm{var}(\kappa_3) &= \frac{15}{N} \sigma^6 \\ \mathrm{var}(\kappa_4) &= \frac{193}{N} \sigma^8 \\ \mathrm{var}(\kappa_5) &= \frac{345}{N} \sigma^{10} \\ \mathrm{var}(\kappa_6) &= \frac{945}{N} \sigma^{12} \\ \mathrm{var}(\kappa_7) &= \frac{16065}{N} \sigma^{14}. \end{aligned} \tag{32}$$

For the purpose of estimating λ and τ the errors can be made small if the number of sampled points N is made large enough. Under our experimental conditions the rms background noise is 0.3 pA at 10 kHz. Given $\lambda = 500$ s^{-1}, $\tau = 1$ μs, and $y_0 = 10$ pA an accumulation of 10^6 data points pushes the error margin for the cumulants below 10% (see Table 1); an rms noise level of 0.4 pA results in errors below 20%.

EXPERIMENTAL

Recordings from microbilayers

Ion currents through gramicidin A channels incorporated into artificial bilayers on pipette tips were recorded and the data stored as described previously (Sigworth et al., 1987; Heinemann and Sigworth, 1990). Filtering of the data consisted of the 10 kHz Bessel filter of the EPC-7 patch clamp, followed by a 17 kHz

TABLE 1 Statistical error estimates for cumulants

Index	Unit	κ_i	S.D. (κ_i)	Deviation (%)
2	A^2	2.1×10^{-27}	1.6×10^{-28}	7.3
3	A^3	1.6×10^{-40}	1.0×10^{-40}	6.7
4	A^4	1.6×10^{-52}	9.6×10^{-53}	2.8
5	A^5	2.2×10^{-63}	1.2×10^{-64}	2.0
6	A^6	3.6×10^{-75}	1.6×10^{-76}	0.6
7	A^7	7.1×10^{-87}	2.8×10^{-89}	0.4

Statistical error estimates for the cumulants κ_i based on the following assumptions: rms background noise = 0.3 pA, number of accumulated data points = 10^6, dwell time of closing events $\tau = 1$ μs, their frequency of occurrence $\lambda = 500$ s^{-1}, single-channel amplitude $y_0 = 10$ pA, and filter frequency $f_c = 10$ kHz. Because λ determines the magnitude of the cumulants linearly, the percent deviation scales inversely with λ.

Butterworth filter in the modified PCM encoder (Sony PCM-701). The membranes were formed from glycerol-monooleate (Nu Chek Prep, Elysian, MN), 40 mg/ml in squalene (Sigma Chemical Corp., St. Louis, MO). As permeant ions we used chloride solutions of NH_4^+ and Cs^+. Optical-grade purified CsCl (Sigma Chemical Co.) was used because we found it enhanced the stability of the membranes.

Open channel noise analysis

Spectra of the open-channel current noise were obtained as previously described (Sigworth, 1985; Heinemann and Sigworth, 1990). Closing events longer than ~10 μs were masked out before calculating the Fourier transform in blocks of 1,024 data points taken at 44.1 kHz sampling rate. The raw spectra were corrected for the transfer function of the recording system.

The masked data blocks were compiled into histograms of 127 bins with a typical bin width of 0.05 pA. Histograms of manually selected regions of the recorded trace were then accumulated, each of them centered at the mean to avoid contaminations due to slight baseline shifts. (This procedure mimicks the application of a high-pass filter with a corner frequency of ~44.1 kHz/1,024 = 43 Hz.) The raw moments up to the eighth order were calculated from these accumulated histograms. These moments were then shifted to moments about the mean and the error introduced by the binning into histograms was corrected by application of Sheppard's formula (Kendall, 1947) as described in the Appendix. The cumulants were then calculated from the moments according to Eqs. 4.

The amplitude distributions of baseline currents were well described by Gaussian functions (see Fig. 5). Their cumulants were subtracted from the cumulants of the open-channel current distribution to yield the cumulants of the open-channel noise only.

RESULTS

Simulated channel noise

To test our numerical implementations and the limits of applicability of the theory we first analyzed simulated data. We simulated an open channel of 10 pA amplitude and superimposed closing events at various rates λ and exponentially distributed dwell times τ. To avoid sampling errors, the generation of these events was performed with an effective sampling rate of 3.2 MHz, then digitally filtered with a 80-kHz Gaussian filter and decimated by a factor of 16. A total of 16×10^6 samples were generated in this way, and analyzed. These data were then filtered to 40 kHz and decimated again by 2. This process of filtering to half the corner frequency and decimating by 2 was repeated to yield data sets down to an effective sampling rate of 12.5 kHz and bandwidth of 2.5 kHz. In most cases a Gaussian background noise was added. Gaussian random numbers, generated with the Box-Muller algorithm and corresponding to 3.0 or 4.0 pA rms were added to the original (3.2 MHz effective sampling rate) data before filtering.

From these sets, moments and cumulants were accumulated and processed as described in the previous section. A set of histograms is shown in Fig. 3 with superimposed Gaussian functions. Each histogram shows skew in the negative (channel closing) direction as expected, with the 80 kHz data extending all the way to −10 pA, corresponding to completely resolved closures. The values for τ and λ estimated from pairs of the cumulants from such histograms are plotted in Fig. 4 as a function of the filter bandwidth, with the various symbols representing estimates obtained from different pairs of cumulants. Part *A* shows the estimates from simulations in which no background noise was added. The accuracy of the predictions was best at 10 kHz bandwidth and using the lowest-order cumulants, κ_2 and κ_3. At this bandwidth a compromise is apparently achieved: with increasing filter bandwidth the cumulants are larger; however, when the duration of the longest gaps approach the filter risetime $T_r \simeq 0.33/f_c$ their amplitude approaches the full channel amplitude y_0. The result is that the first term in the Taylor expansion (Eq. 13) fails to be a good approximation to the time course of the response to these events. This leads to a systematic underestimation of τ and an overestimation of λ.

In Fig. 4, *B* and *C*, white background noise was added to the simulated signal, resulting in a standard deviation of 0.25 pA at f_c = 10 kHz. This was much larger than the ~0.01 pA standard deviation of the noise from the gaps. It can be seen that the lowest-order cumulants did not always give the most reliable estimates for τ and λ under these conditions, a trend that is also reflected in the error estimates in Table 1. From the simulations it can be concluded that under the conditions the maximum accuracy is obtained for a filter frequency close to 10 kHz for events of 1.5 μs and 20 kHz for events of 1.0 μs duration. In theses cases the estimates for τ and λ do not depend strongly on the order of the cumulants used for the calculation.

Experimental data

In Fig. 5 examples of experimental current histograms are plotted semilogarithmically. From the calculated mean, variance, and the area of each histogram, matching Gaussian functions were computed and are shown

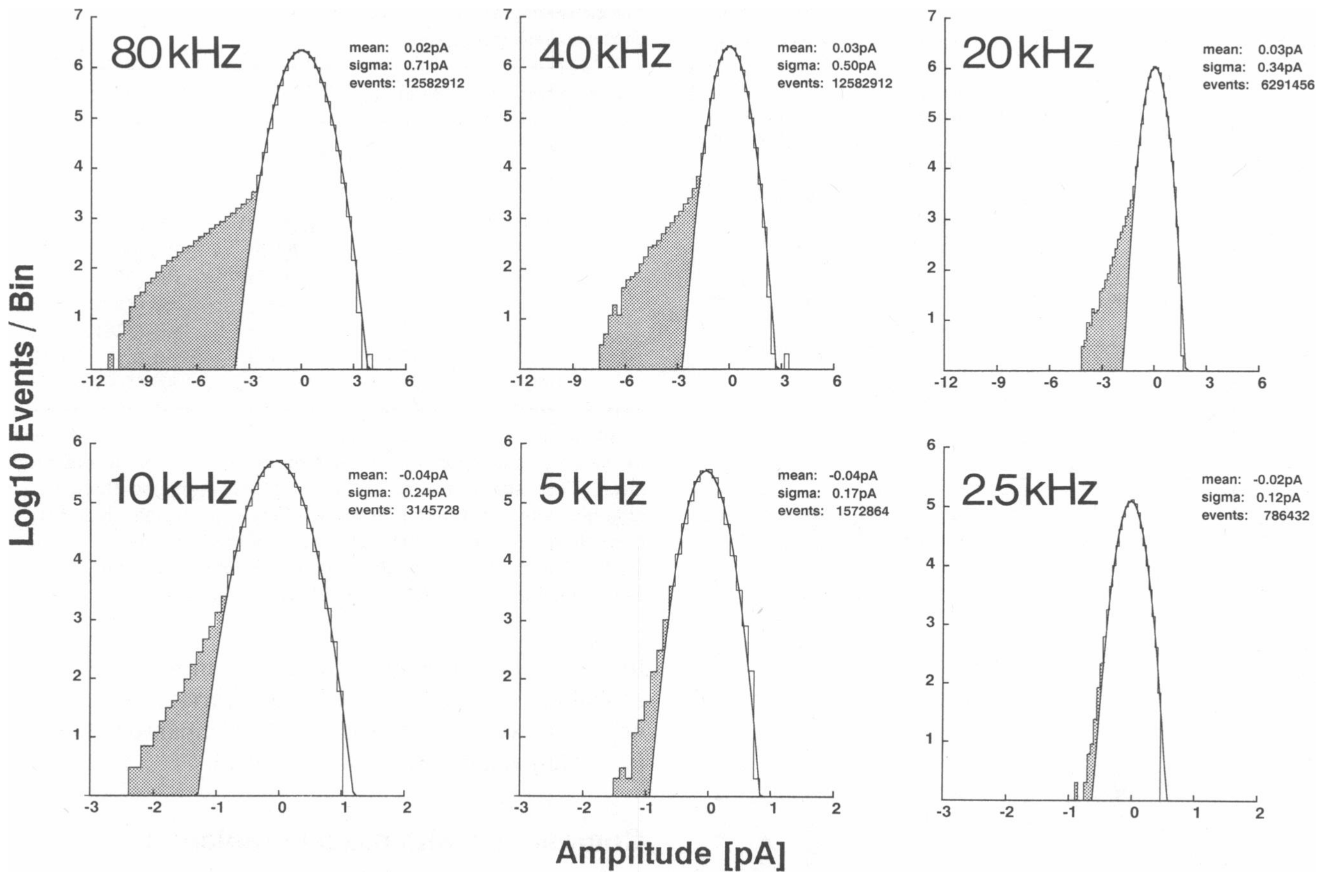

FIGURE 3 Amplitude histograms from simulated 10 pA channel currents with brief gaps. The simulated currents with added Gaussian noise were filtered to the bandwidths shown. The accumulation of histograms shifted the origin of each to the mean, so that resolved channel closures appear as points near −10 pA. The shaded regions indicate the deviations of the histograms from Gaussian; histograms are drawn on a $\log_{10}$ scale to make these small residuals visible. The closing events were simulated with the parameters $\tau = 0.94$ μs and $\lambda = 800\ s^{-1}$. Independent Gaussian noise samples (3.0 pA rms) were added to the simulated channels at the original 3.2 MHz effective sampling rate; this resulted in ~0.2 pA rms noise at 10 kHz bandwidth.

superimposed. The lower of each pair of histograms was compiled from stretches of baseline; the Gaussian curves match these histograms well. In the case of NH_4^+ as permeating ion (Fig. 5 *A*) the open-channel (*upper*) histograms are also well described by Gaussian functions. The histograms compiled from currents in CsCl, however, display large deviations from a Gaussian in the negative (i.e., channel-closing) direction. The one-sided skew is consistent with the presence of brief closures which could not be eliminated by the masking procedure, i.e., they must be shorter than ~10 μs.

In contrast to the emulated data we cannot predict a priori what the background noise is in experimental data. As described above, we simply subtracted the cumulants of baseline currents from the cumulants of the open-channel current distributions. But then there is the high-frequency ion-transport noise. As discussed above, we assume that this noise is Gaussian, and therefore will contribute only to κ_2 and not to the higher-order cumulants. To the extent that this noise is not sufficiently filtered to be truly Gaussian, it will make a relatively larger contribution to the lower-order cumulants than to the higher-order ones. This can be understood from Eq. 21 where the size of κ_n is seen to be of the order of τ^n.

Fig. 6 presents estimates of τ and λ computed from Eqs. 22 and 23 as a function of the order of the cumulants used in the calculation. Also plotted in the figure (*squares*) are corresponding estimates from the simulated data of Fig. 4 *B* obtained at the same 10 kHz bandwidth. In the simulation the estimates for τ and λ were quite insensitive to which order of cumulants was used, but the experimental data show a trend toward higher τ values with higher orders. The τ values obtained from the ratio κ_3/κ_2 (i.e., index 3) are expected to be low because κ_2 includes a large contribution from the nearly

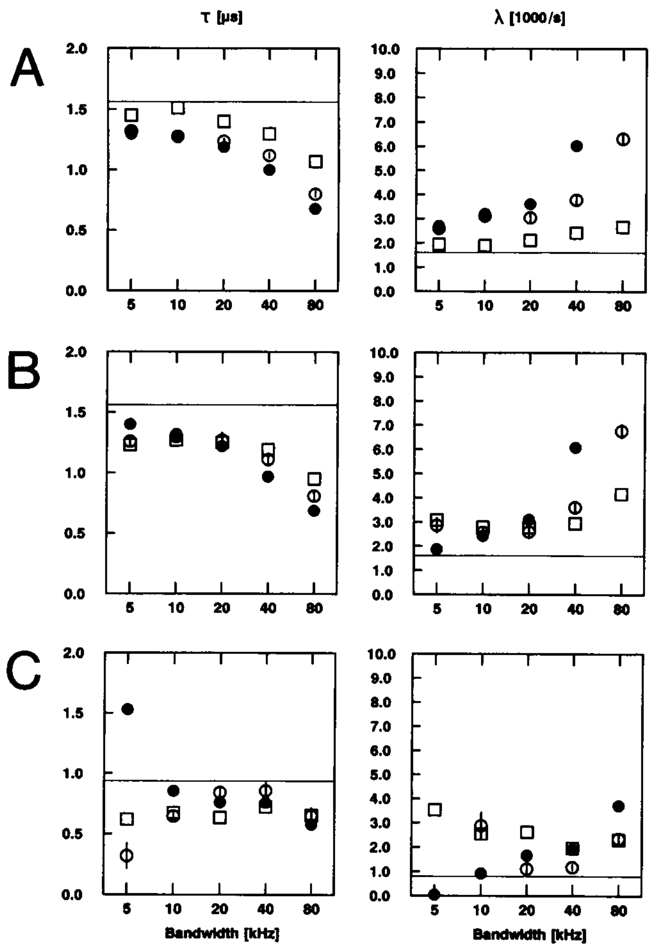

FIGURE 4 Estimates of τ and λ from simulated data as in Fig. 3, plotted as a function of filter bandwidth. Horizontal lines show the values used in the simulations. (*A*) Values obtained from simulated data without background noise and with $\tau = 1.56$ μs, $\lambda = 1{,}600$ s^{-1}. (*B*) Estimates from simulated data with the same parameters but with background noise of 3.0 pA rms (at 3.2 MHz) added. (*C*) Estimates from simulated data with background noise of 3.0 pA rms at 3.2 MHz, $\tau = 0.94$ μs, and $\lambda = 800$ s^{-1}. Estimates of τ and λ were calculated using different pairs of cumulants as indicated by the symbols: κ_2 and κ_3 (*squares*); κ_3 and κ_4 (*open circles*, with the theoretical standard errors from Table 1 shown as bars); and κ_4 and κ_5 (*solid circles*).

Gaussian high-frequency transport noise as well. That the estimate from index 4 is also relatively low suggests that κ_3 might also be contaminated by nonGaussian components of the high-frequency transport noise. The experimental estimates converge, however, for index 5 and above.

Analysis of the cumulants of these and other histograms from Cs^+ currents yielded estimates for the τ near 1.0 μs, while λ varied between ~50 and 1,000 s^{-1}. Estimates were obtained for these parameters by averaging the values obtained at orders 5 (i.e., from κ_4 and κ_5) through 7, and are summarized in Table 2. The origin of

TABLE 2 **Estimates of τ and λ for Cs^+ currents in GMO/squalene membranes**

Concentration	Potential	τ	λ	N
mmol/l	*mV*	*μs*	s^{-1}	
1,280	100	1.09 (6)	569 (192)	4
	200	0.69 (5)	537 (273)	3
640	100	1.34 (12)	50 (38)	3
	200	0.79 (6)	188 (60)	1
	300	0.65 (7)	486 (260)	2
320	100	1.25 (3)	58 (8)	1
	200	1.07 (8)	836 (328)	1
	400	1.24 (8)	91 (53)	3
160	200	2.33 (78)	1909 (1869)	1

Estimates for τ and λ by analysis of open-channel current histograms for various concentrations of CsCl and at the membrane potentials given. The estimates were obtained by averaging the three values obtained with κ_5 through κ_7 from N different recordings. Numbers in parentheses give the standard deviations of the last significant figures; for $N = 1$ the standard deviations are those computed among the three values obtained with different cumulants for the single run.

the large variation in λ values is unknown, but it is probably related to the rather large variations in current noise that we observed with Cs^+ as compared with other ions (Heinemann and Sigworth, 1990).

Comparison with model predictions

In the five-state model of Fig. 2*A* the mean dwell time τ in the blocked state [00]* is expected to be

$$\tau = \frac{1}{\beta_0^{-1} + 2f_1^*[\mathrm{Cs}]\cosh(\delta e_0 V/2kT)}, \tag{33}$$

where $\delta/2$ is the relative electrical distance of the activation barrier for the ion binding step whose rate, at membrane potential $V = 0$, is f_1^*. The scheme predicts that τ decreases with increasing membrane potential and ion concentration, as is observed (Table 2).

In our previous analysis the values of τ and λ were poorly constrained by the data; we nevertheless estimated τ_0 to be 3.0 μs and, for Cs^+, f_1^* was 4.1×10^6 and δ was 0.074. The resulting τ values at $V = 200$ mV ranged from 0.6 μs at [Cs] = 160 mM to 0.1 μs at [Cs] = 1,280 mM. The values listed in Table 2 are larger than these by factors of 4–7. We therefore performed new fits to the kinetic scheme to see what other sets of rate constants

FIGURE 5 Open-channel and baseline current histograms from GA channels in (*A*) NH_4Cl, and (*B*) CsCl solutions of the concentrations shown. The baseline histograms (lower of each pair) are well described by Gaussian functions. The open-channel current histogram for NH_4Cl solutions are also essentially Gaussian, but the CsCl open-channel currents have substantial tails. Histograms were compiled from numbers of samples between 3.1×10^5 and 3.3×10^6.

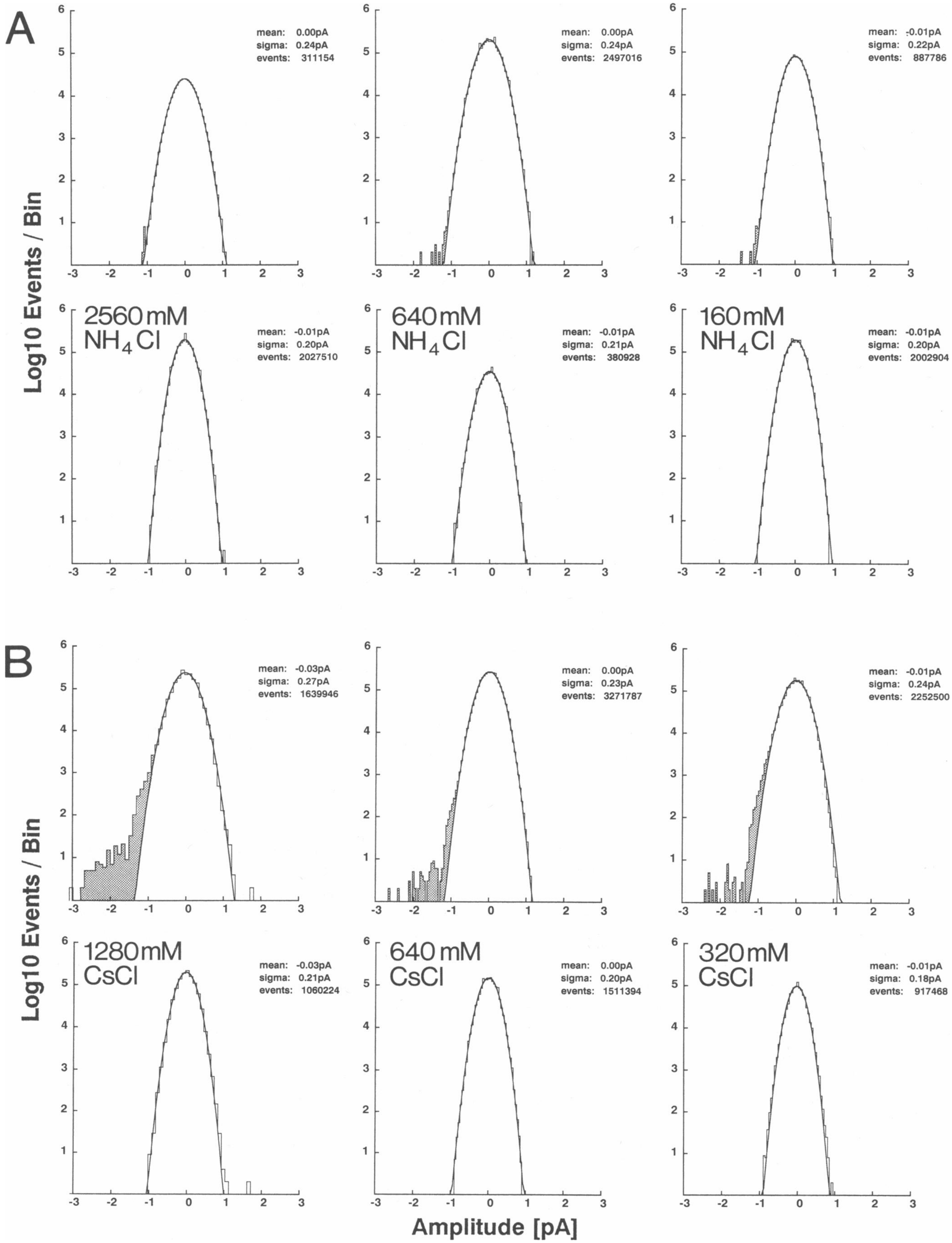
A
mean: 0.00pA
sigma: 0.24pA
events: 311154
mean: 0.00pA
sigma: 0.24pA
events: 2497016
mean: -0.01pA
sigma: 0.22pA
events: 887786
2560 mM
NH4Cl
mean: -0.01pA
sigma: 0.20pA
events: 2027510
640 mM
NH4Cl
mean: -0.01pA
sigma: 0.21pA
events: 380928
160 mM
NH4Cl
mean: -0.01pA
sigma: 0.20pA
events: 2002904
B
mean: -0.03pA
sigma: 0.27pA
events: 1639946
mean: 0.00pA
sigma: 0.23pA
events: 3271787
mean: -0.01pA
sigma: 0.24pA
events: 2252500
1280 mM
CsCl
mean: -0.03pA
sigma: 0.21pA
events: 1060224
640 mM
CsCl
mean: 0.00pA
sigma: 0.20pA
events: 1511394
320 mM
CsCl
mean: -0.01pA
sigma: 0.18pA
events: 917468
Log10 Events / Bin
Amplitude [pA]

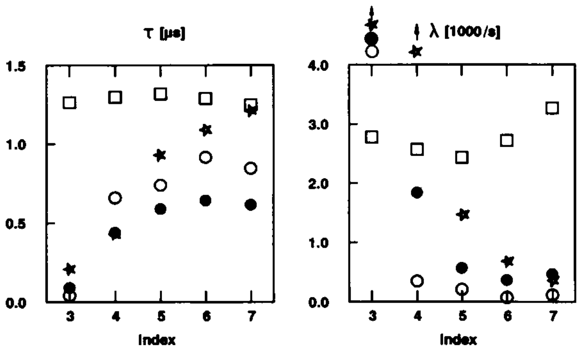

FIGURE 6 Estimates of τ and λ for currents in 320 mM, CsCl (*stars*), 640 mM CsCl (*open circles*) and 1,280 mM CsCl (*solid circles*). The index value i means that κ_i and κ_{i-1} were used in the evaluation. The estimates appear to converge for the higher orders. For comparison, the squares show corresponding values obtained from the 10 kHz-filtered, simulated data with $\tau = 1.56$ μs and $\lambda = 1{,}600\ s^{-1}$ (same as in Fig. 4 *B*).

were compatible with the spectral density data of our previous study (Heinemann and Sigworth, 1990). Increasing τ_0 to 5 μs, reducing f_1^* to $1.4 \times 10^6\ s^{-1}\ M^{-1}$, and reducing λ fivefold to 7,000 s^{-1} resulted in data fits that were essentially as good as those with the previous values. Further, the spectral data for the other ions could also be well fitted with the new values for τ and λ. With these parameters the gap times associated with sojourns in [00]* are 1.5 μs at [Cs] = 160 mM and 0.3 μs at [Cs] = 1,280 mM.

DISCUSSION

In our previous paper (Heinemann and Sigworth, 1990) we reported a substantial excess noise in currents through GA channels carried by Cs^+ and K^+ but not by Na^+ or NH_4^+. The concentration dependence of the fluctuations could be accounted for by a model in which the energy barriers to ion entry can fluctuate. In a kinetic model (see Fig. 2 *A*) the fluctuations are represented as transitions to a "blocked" channel state [00]*, which can be accessed via the empty channel configuration [00]. The model predicts interruptions of the open-channel current, representing sojourns in the state [00]*, having a mean duration on the order of 1 μs and occurring at a rate of $\sim 10^4$ per second times the probability that the channel is empty.

The goal of the present work was to search for evidence of such gaps in the channel current and to estimate their kinetics. Our approach is to analyze the amplitude distribution of the recorded channel current by computing the cumulants. On the basis of the theory presented here, it is possible to estimate the duration and rate of gaps by comparing pairs of cumulant values. The theory is valid in the limit that the gap durations are much shorter than the response time of the recording system, and also that the gap durations are shorter than the inter-gap intervals. From simulations we see that the theory is in fact successful in estimating gap durations of ~1 μs for data filtered at 10 kHz, but the method would encounter substantial systematic errors for event durations longer than 5–10 μs. Thus our theory can be considered as complementary to that of FitzHugh (1983). He presented the exact form of the amplitude distribution of channel currents filtered with a simple first-order filter; this solution has turned out to be useful in analyzing Bessel-filtered data as well, in cases where the underlying events border on being resolvable, i.e., have dwells on the order of the filter risetime (Yellen, 1984).

The contribution of brief gaps to amplitude distributions is seen to be very small tails that are skewed in the direction of channel closing. Large numbers of samples (typically 10^6 in our case) are required to obtain good estimates of the cumulant values, and the experimental histograms could easily be distorted by slower processes and unmasked longer closures. Our confidence in the analysis presented here of the GA channel currents is strengthened by the following observations. First, the histograms of "background" noise obtained from channel-closed intervals are nearly perfect Gaussians. Secondly, the open-channel current distribution with NH_4^+ as the charge carrier is also nearly Gaussian. From our analysis of spectral density in the previous paper we had predicted that the dwell time in the state [00]* would be very short for NH_4^+ and that the open-channel noise would be essentially the rapid ion-transport noise alone. Thirdly, with the Cs^+ current data, internally consistent estimates are obtained for λ and τ using different pairs of cumulants with orders of 4 to 7.

Our analysis therefore supports the idea from our previous paper that currents in GA have excess noise that arises from brief interruptions in the channel current. The values we estimate here for the gap duration are ~5 times larger than those obtained from curve-fitting in the previous study, but fall within the range of values that can fit the spectral-density data from that work.

APPENDIX

Calculation of moments from a discrete distribution

Raw moments

The moments of a distribution about the value zero are defined as

$$\mu'_n = \int_{\infty}^{-\infty} x^n f(x)\, dx \qquad (34)$$

with the distribution function, $f(x)$, However, experimentally only a discrete distribution is determined. Let the distribution be compiled in bins of length h; the magnitude of the bin centered around x_i is

$$f_i = \int_{-h/2}^{h/2} f(x_i + \xi)\, d\xi. \tag{35}$$

The measured raw moments, denoted by a bar, are therefore

$$\overline{\mu}'_n = \sum_{i=-\infty}^{\infty} x_i^n f_i. \tag{36}$$

Sheppard's bin correction

Assuming that $f(x)$ decays monotonically to zero at the edges of the distribution, the "true" moments can be calculated with Sheppard's correction formula (Kendall, 1947)

$$\mu'_n = \sum_{i=0}^{n} \left\{ \binom{n}{i} (2^{1-i} - 1)\beta_i h^i \overline{\mu}'_{n-i} \right\}. \tag{37}$$

The β_i are Bernoulli's numbers of ith order: $\beta_i = 0$ for odd i; $\beta_2 = 1/6$, $\beta_4 = -1/30$, $\beta_6 = 1/42$, etc.

We thank Dr. A. G. Hawkes for pointing out the applicability of cumulants to this problem, and Dr. E. Neher for helpful comments on the manuscript.

Dr. Sigworth's support was provided by National Institutes of Health grant NS-21051.

Received for publication 10 December 1990 and in final form 29 April 1991.

REFERENCES

Andersen, O. S. 1984. Gramicidin channels. *Annu. Rev. Physiol.* 46:531–548.

Campbell, N. 1909. The study of discontinuous phenomena. *Proc. Cambr. Phil. Soc.* 15:117–136.

Colquhoun, D., and D. C. Ogden. 1988. Activation of ion channels in the frog end-plate by high concentrations of acetylcholine. *J. Physiol. (Lond.).* 395:131–159.

Colquhoun, D., and F. J. Sigworth. 1983. Fitting and statistical analysis of single-channel records. *In* Single-Channel Recording. B. Sakmann and E. Neher, editors. Plenum Publishing Corp., New York. 191–263.

Fesce, R., J. R. Segal, and W. P. Hurlbut. 1986. Fluctuation analysis of nonideal shot noise. Application to the neuromuscular junction. *J. Gen. Physiol.* 88:25–57.

Finkelstein, A., and O. S. Andersen. 1981. The gramicidin A channel: a review of its permeability characteristics with special reference to the single-file aspect of transport. *J. Membr. Biol.* 59:155–171.

FitzHugh, R. 1983. Statistical properties of the asymmetric random telegraph signal, with applications to single-channel analysis. *Math. Biosci.* 64:75–89.

Frehland, E. 1978. Current noise around steady states in discrete transport systems. *Biophys. Chem.* 8:255–265; 10:128.

Frehland, E. 1982. Stochastic Transport Processes in Discrete Biological Systems. Lecture Notes in Biomathematics, vol. 47. Springer-Verlag, Berlin. 103–117.

Heinemann, S. H., and F. J. Sigworth. 1988. Open channel noise. IV. Estimation of rapid kinetics of formamide block in gramicidin A channels. *Biophys. J.* 54:757–764.

Heinemann, S. H., and F. J. Sigworth. 1989. Estimation of Na^+ dwell time in the Gramicidin A channel. Na ions as blockers of H^+ currents. *Biochim. Biophys. Acta.* 987:8–14.

Heinemann, S. H., and F. J. Sigworth. 1990. Open channel noise. V. Fluctuating barriers to ion entry in gramicidin A channels. *Biophys. J.* 57:499–514.

Kendall, M. G. 1947. The advanced theory of statistics. Charles Griffin & Company, London. 49–74.

Läuger, P. 1978. Transport noise in membranes. Current and voltage fluctuations at equilibrium. *Biochim. Biophys. Acta.* 507:337–349.

Nyquist, H. 1928. Thermal agitation of electric charge in conductors. *Physical Review.* 32:110–113.

Pietrobon, D., B. Prod'hom, and P. Hess. 1989. Interactions of protons with single open L-type calcium channels. pH dependence with Cs^+, K^+, and Na^+ as permeant ions. *J. Gen. Physiol.* 94:1–21.

Rice, S. O. 1954. Mathematical analysis of random noise. *In* Selected Papers on Noise and Stochastic Processes. N. Wax, editor. Dover Publications Inc., New York. 133–183

Sandblom, J., G. Eisenman, and J. Hägglund. 1983. Multioccupancy models for single-filing ionic channels: theoretical behavior of a four-site channel with three barriers separating the sites. *J. Membr. Biol.* 71:61–78.

Sigworth, F. J. 1985. Open channel noise. I. Noise in acetylcholine receptor currents suggests conformational fluctuations. *Biophys. J.* 47:709–720.

Sigworth, F. J., D. W. Urry, and K. Prasad. 1987. Open channel noise. III. High-resolution recordings show rapid current fluctuations in gramicidin A and four analogues. *Biophys. J.* 52:1055–1064.

Sine, S. M., T. Claudio, and F. J. Sigworth. 1990. Activation of *Torpedo* acetylcholine receptors expressed in mouse fibroblasts. Single channel current kinetics reveal distinct agonist binding affinities. *J. Gen. Physiol.* 96:395–437.

Urban, B. W., S. B. Hladky, and D. A. Haydon. 1980. Ion movements in gramicidin pores. An example of single-file transport. *Biochim. Biophys. Acta.* 602:331–354.

Yellen, G. 1984. Ionic permeation and blockade in Ca^{2+}-activated K^+ channels of bovine chromaffin cells. *J. Gen. Physiol.* 84:157–186.